

# Sulphonated Carbon Dots-Chitosan hybrid hydrogel nanocomposite as an efficient ion-exchange film for $\text{Ca}^{2+}$ and $\text{Mg}^{2+}$ removal

*Upama Baruah<sup>a</sup>, Achyut Konwar<sup>a</sup> and Devasish Chowdhury<sup>a\*</sup>*

*<sup>a</sup>Material Nanochemistry Laboratory, Physical Sciences Division, Institute of Advanced Study in*

*Science and Technology, Paschim Boragaon, Garchuk, Guwahati, 781035, India. E-mail:*

*devasish@iasst.gov.in; Fax: +91 361 2279909; Tel: +91 361 2912073*

## **ELECTRONIC SUPPLEMENTARY INFORMATION**

### **Experimental Section**

#### **Materials**

11-Mercaptoundecanoic acid was purchased from Sigma Aldrich. Sodium hydroxide flakes, hydrogen peroxide solution 50% (purified), acetic acid (glacial) 99-100% for synthesis, glycerol (anhydrous)  $\geq 98\%$ , calcium chloride were purchased from Merck India Limited. Chitosan (M.W. 193400), was purchased from Sisco Research Laboratories Pvt. Ltd., India.

#### **Instrumentation**

Particle size and zeta potential measurements were carried out on a Malvern Zetasizer Nanoseries, Nano-ZS90. SEM images were collected on a Carl Zeiss Sigma VP instrument. Powder XRD spectrum was collected on a Bruker D8 Advance diffractometer. The TGA thermograms were recorded in Perkin Elmer 4000 in the temperature range of 35–800°C at a

heating rate of 10°C/min under nitrogen flow rate of 20 ml/min. Centrifugation was carried out on a Spinwin microcentrifuge. UV-Visible absorption spectra were collected on a Shimadzu UV-VIS Spectrophotometer, UV-2600, Optics Technology UV lamp (365 nm) was used to check fluorescence intensity of CDs, PL emission spectra were collected on a Jasco Specfluorometer FP-8300, Fourier Transform Infrared Spectra (FTIR) were collected on a Nicolet-6700 FT-IR Spectrophotometer and Atomic Absorption Spectroscopy was carried out on a Shimadzu AA-7000 Atomic Absorption Spectrophotometer.

### **1. Synthesis of Carbon Dots from 11-Mercaptoundecanoic acid (MUA)**

Blue photoluminescent carbon dots were prepared from 11-Mercaptoundecanoic acid. In this work for the first time we introduce 11-Mercaptoundecanoic acid as a novel carbon source for carbon dots synthesis. Briefly, 0.1g of MUA was taken in a beaker and heated at 250°C for 45 minutes. The solid mass melted into a colorless liquid which gradually turned yellow, then orange and finally dark brown in color. The brown liquid so obtained was then added dropwise to 10 mL of 1.25 M NaOH solution under vigorous stirring. This solution was then centrifuged at 7000 rpm for 30 minutes. The supernatant solution containing the fluorescent carbon dots was collected and characterized and named as MUA-SH-CDs.

### **2. Oxidation of Carbon Dots synthesized from 11-Mercaptoundecanoic acid**

For oxidation of MUA-SH-CDs prepared, 10 mL of MUA-SH-CDs solution was taken in a beaker and to it 5 mL of 30% H<sub>2</sub>O<sub>2</sub> solution was added and stirred magnetically for 3 hours at room temperature. The original brown color of the CDs solution gradually fades away along with the evolution of effervescence. The resulting solution obtained was the oxidized CDs solution and was named as MUA-SO<sub>3</sub>Na-CDs.

### **3. Characterization of Carbon Dots (CDs) prepared from MUA before and after oxidation**

The CDs prepared from MUA and subsequently oxidized with H<sub>2</sub>O<sub>2</sub> were subjected to extensive characterization by various analytical techniques viz. Dynamic Light Scattering measurements, Scanning Electron Microscopy, UV-Visible spectroscopy, IR Spectroscopy, Fluorescence spectroscopy and Powder XRD Analysis.

*3.1 Inference from Dynamic Light Scattering (DLS) and Scanning Electron Microscopy (SEM) Analysis*

The particle size and zeta potential of the carbon dots synthesized from MUA were determined both before and after oxidation using Dynamic Light Scattering Technique. Figure S1 (A) and (C) show the particle size graphs and zeta potential values of the CDs before and after oxidation. The particle sizes of the CDs were found to be below 10 nm. Further, the zeta potential of the CDs (-34.266 mV) was found to become more negative (-52.233 mV) after oxidation. This is quite obvious due to incorporation of oxygenated sulphonate groups which confirms the successful oxidation of -SH groups on the CDs to -SO<sub>3</sub><sup>-</sup> groups upon oxidation with H<sub>2</sub>O<sub>2</sub>. In order to ascertain the presence of particles below 10 nm, SEM images of CDs were recorded both before and after oxidation. Figure S1 (B) and (D) show the SEM micrographs of the CDs before and after oxidation.

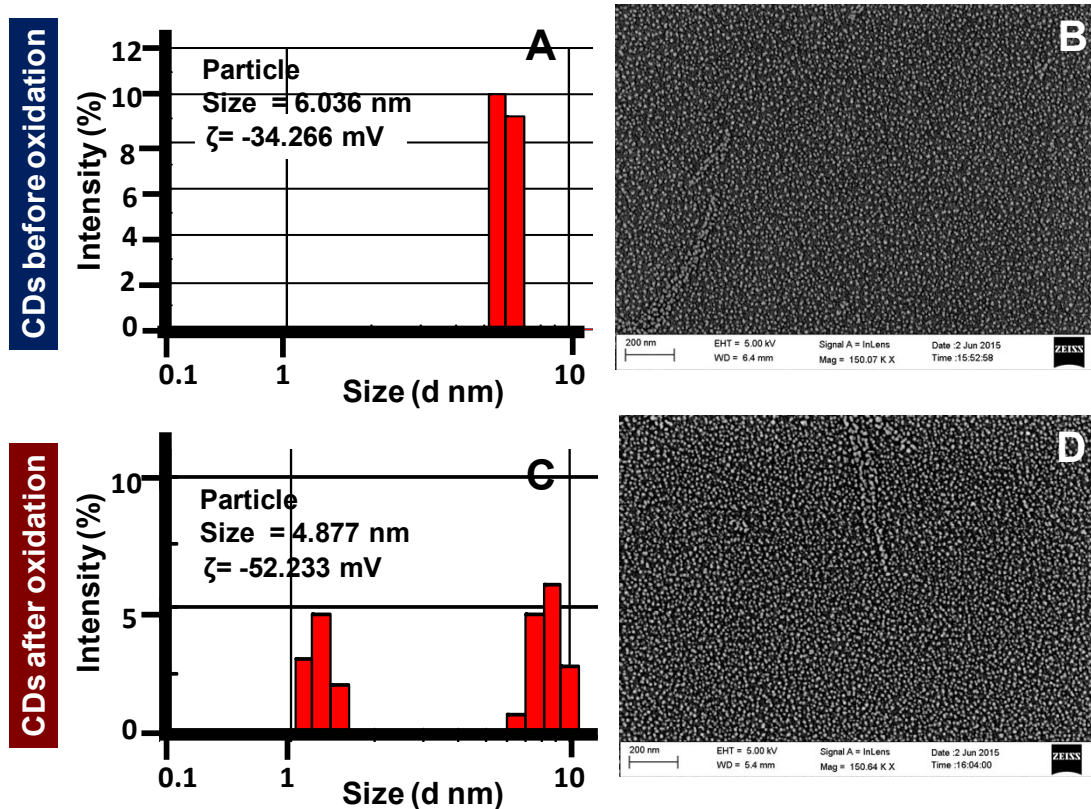


**Figure S1.** (A) Particle size graph and zeta potential value of CDs prepared from MUA (B) SEM micrograph of CDs with -SH surface functionality before oxidation (C) Particle size graph and zeta potential value of CDs and (D) SEM micrograph of CDs with -SO<sub>3</sub><sup>-</sup> surface functionality after oxidation.

Interestingly, the SEM micrographs too revealed the presence of particles below 10 nm in diameter. Thus, it can be said that the CDs prepared from MUA were of size below 10 nm as evident from DLS and SEM analysis. Furthermore, the evidence for the fact that the prepared carbon dots possess sulfur-containing groups on the surface can be drawn from the EDX spectrum of the CDs. Figure S2 (A) shows the EDX Spectrum of CDs prepared from MUA and Table 1 shows the respective weight percentages of different elements present.

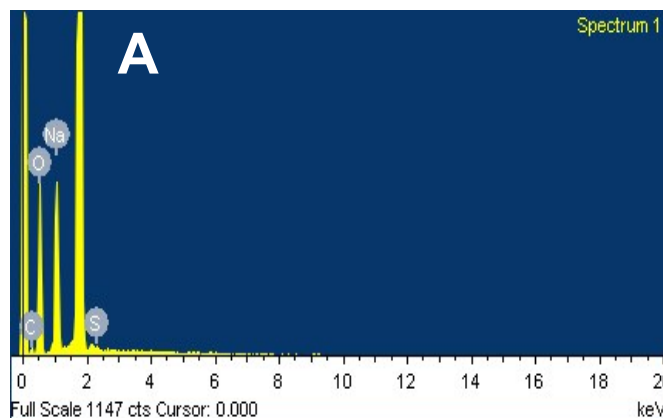


**Table 1:** the respective weight percentages of different elements present in the CDs

Element	Weight %	Atomic %
C	10.026	14.03
O	57.793	61.11
Na	31.913	24.57
S	0.273	0.29
<b>Total</b>	<b>100.00</b>	

**Figure S2.** (A) The EDX Spectrum of CDs prepared from MUA and Table 1 shows the respective weight percentages of different elements present.

### 3.2 Inference from UV-Visible and FTIR Spectroscopic Analysis

In order to ascertain the presence of surface functionalities on the CDs, UV-Visible and FTIR Spectra of the CDs were recorded both before and after oxidation of CDs. Figure S3 (A) shows the comparative UV-Visible spectra of the CDs both before and after oxidation.

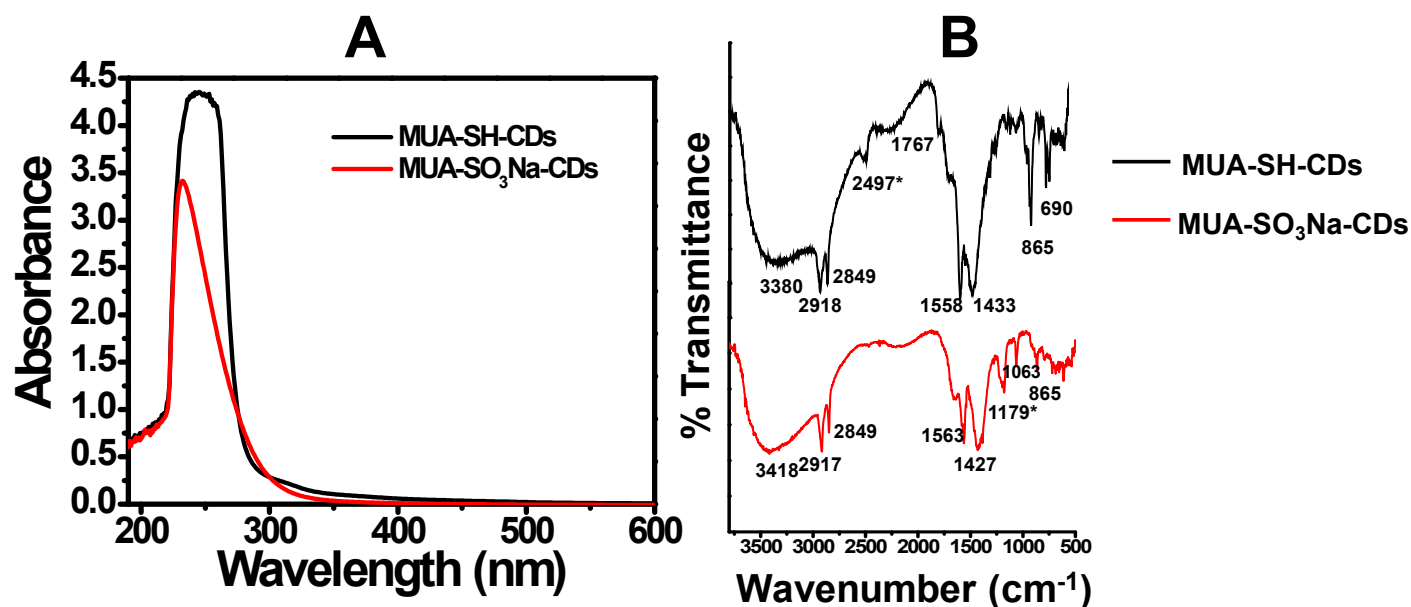


**Figure S3.** (A) The comparative UV-Visible spectra and (B) the comparative FTIR spectra of the CDs before and after oxidation.

From the UV-Visible spectra it is evident that the MUA-SH-CDs exhibit an absorption peak at 245 nm owing to the  $n-\pi^*$  transitions of the  $-\text{COOH}$  groups on the CDs prepared from MUA. Upon oxidation of CDs with  $\text{H}_2\text{O}_2$ , this characteristic absorption peak was found to be hypsochromically shifted to 231 nm which can be attributed to the increased electron density ( $\pi-\pi^*$  transitions of  $-\text{COO}^-$  and  $-\text{SO}_3^-$  groups) on the CDs due to oxidation of the  $-\text{SH}$  groups to  $-\text{SO}_3^-$  groups. Figure S2 (B) shows the comparative FTIR spectra of the CDs both before and after oxidation. The characteristic peaks appearing in the FTIR spectra of MUA-SH-CDs and MUA- $\text{SO}_3\text{Na}$ -CDs and the corresponding peak assignments showing the successful oxidation of MUA-SH-CDs to MUA- $\text{SO}_3\text{Na}$ -CDs are tabulated in Table 2.

From the table it is to be observed that the peak appearing at  $2497\text{ cm}^{-1}$  (S-H stretch) for MUA-SH-CDs was not present in the FTIR spectrum of MUA- $\text{SO}_3\text{Na}$ -CDs. Further, the peak appearing at  $1179\text{ cm}^{-1}$  (S=O stretch sulfonates) for MUA- $\text{SO}_3\text{Na}$ -CDs was absent for MUA-SH-CDs. This is a clear indication of the successful oxidation of the  $-\text{SH}$  groups of MUA-SH-CDs to  $-\text{SO}_3\text{Na}$  groups in MUA- $\text{SO}_3\text{Na}$ -CDs.

**Table 2.** The characteristic peaks appearing in the FTIR spectra of MUA-SH-CDs and MUA- $\text{SO}_3\text{Na}$ -CDs and the corresponding peak assignments.

MUA-SH-CDs	MUA- $\text{SO}_3\text{Na}$ -CDs	Peak Assignment
3380	3418	O-H stretch carboxylic acid
2918, 2849	2917, 2849	C-H stretch alkanes
2497	absent	S-H stretch
1767	absent	C=O stretch carboxylic acid
1558	1563	
1433	1427	C-H bend alkanes

absent	1179	S=O stretch sulfonates
865	865	C-H rock alkanes

### 3.3 Inference from Photoluminescence (PL) Spectroscopic Analysis

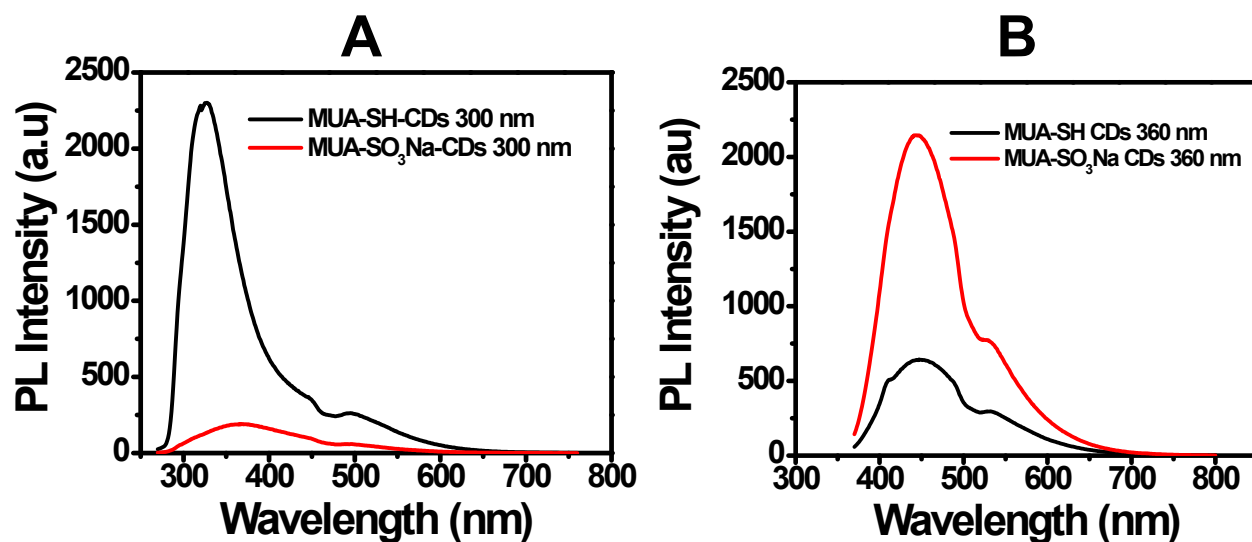


**Figure S4.** The comparative PL emission spectra of CDs before and after oxidation at two different excitation wavelengths viz. at (A) 300 nm and (B) 360 nm.

As the CDs prepared from MUA were of size below 10 nm, they were found to exhibit strong blue fluorescence as observed under a UV-lamp at 365 nm wavelength. Figure S4 shows the comparative PL emission spectra of CDs before and after oxidation at two different excitation wavelengths viz. at (A) 300 nm and (B) 360 nm.

The PL emission spectra of CDs revealed that the prepared CDs exhibit strong excitation dependent emission property. However, the maximum PL emission intensity was observed at different excitation wavelengths for MUA-SH-CDs and MUA-SO<sub>3</sub>Na-CDs. As evident from Figure S4 (A), the emission intensity was found to be higher for MUA-SH-CDs at  $\lambda_{\text{exc}} = 300$  nm and that it was higher for MUA-SO<sub>3</sub>Na-CDs at  $\lambda_{\text{exc}} = 360$  nm. PL analysis therefore provides evidence for the fact that the CDs were fluorescent both before and after oxidation and that fluorescence is a characteristic property of CDs.

#### **4. Fabrication of Chitosan-MUA-SO<sub>3</sub>Na-CDs nanocomposite thin films (Ch-SO<sub>3</sub>Na-CDs films)**

After successful oxidation of MUA-SH-CDs, the oxidized CDs were embedded into a hybrid platform in the form of a nanocomposite thin film via its conjugation with the biopolymer chitosan by forming a hydrogel. Briefly, 0.1g of chitosan was dissolved in 10 mL of a mixture of 2 parts glycerol and 3 parts 0.1 M acetic acid under stirring at room temperature for 2 hours. After complete dissolution of chitosan in the solvent mixture, 6 mL of MUA-SO<sub>3</sub>Na-CDs solution was added dropwise to this solution. Immediately, a hydrogel material began to separate out from the liquid mixture. The beaker containing the hydrogel and the solvent mixture was allowed to stand overnight to ensure complete gel formation. This material formed via conjugation of CDs to chitosan was named as Ch-SO<sub>3</sub>Na-CDs hydrogel. Subsequently, the Ch-SO<sub>3</sub>Na-CDs hydrogel material was filtered and washed thoroughly with milli pore water to remove all the impurities. The hydrogel was then spread onto glass slides and dried in an oven for 2 hours at 50°C. Finally the dried hydrogel films were peeled off from the slides and stored under dessication for further characterization.

#### **5. Fabrication of blank chitosan thin films (Ch-films)**

For control experiments blank chitosan thin films were fabricated and characterized. Typically, 0.1g of chitosan was dissolved in 10 mL of a mixture of 2 parts glycerol and 3 parts 0.1 M acetic acid under stirring at room temperature for 2 hours. After complete dissolution of chitosan in the solvent mixture, 6 mL of 1.25 M NaOH was added dropwise. Immediately, a hydrogel material began to separate out from the liquid mixture. The beaker containing the hydrogel and the solvent mixture was allowed to stand overnight to ensure complete gel formation. It is to be noted that the same procedure is being followed for formation of blank chitosan hydrogel except that 1.25 M NaOH solution is used instead of MUA-SO<sub>3</sub>Na-CDs solution for hydrogel formation as in the previous case. The chitosan hydrogel (Ch-hydrogel) was filtered and washed thoroughly with milli pore water to remove all the impurities. The hydrogel was then spread onto glass slides and dried in an oven for 2 hours at 50°C. Finally the dried hydrogel films were peeled off from the slides and stored under dessication for further characterization.

#### **6. Characterization and comparative analysis of Ch-SO<sub>3</sub>Na-CDs and Blank Ch-films**

*6.1 Inference from ATR Spectroscopy and Thermogravimetric Analysis (TGA)*

The prepared thin films viz. Ch-SO<sub>3</sub>Na-CDs and Blank Ch-films were subjected to ATR Spectroscopic analysis and Thermogravimetric Analysis. Figure S5 (A) shows the comparative ATR spectra of Ch-SO<sub>3</sub>Na-CDs and Blank Ch-films. The characteristic peaks appearing in the ATR spectra of Ch-SO<sub>3</sub>Na-CDs nanocomposite films and for Blank Ch-films and the corresponding peak assignments showing the successful incorporation of MUA-SO<sub>3</sub>Na-CDs into the chitosan hydrogel matrix are tabulated in Table 3.

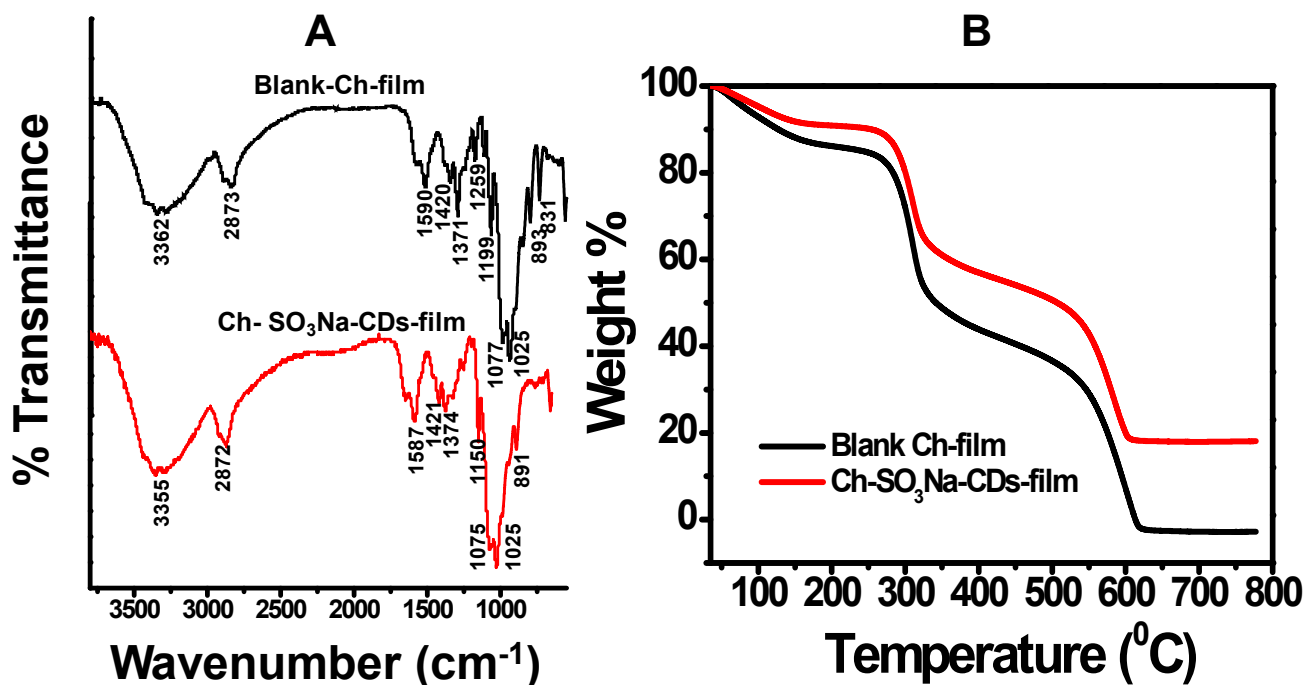


**Figure S5.** (A) Comparative ATR spectra of Ch-SO<sub>3</sub>Na-CDs films and Blank Ch-films (B) Stacked TGA thermograms of Ch-SO<sub>3</sub>Na-CDs and Blank Ch-films.

**Table 3.** The characteristic peaks appearing in the ATR spectra of Ch-SO<sub>3</sub>Na-CDs nanocomposite films and for Blank Ch-films and the corresponding peak assignments.

Blank Ch-film	Ch-SO <sub>3</sub> Na-CDs nanocomposite film	Peak Assignment
3362	3355	O-H stretch Hydrogen bonded
2873	2872	C-H stretch alkanes
1590	1587	



1420	1421	
1371	1374 (reduced intensity)	
1259	absent	
1199	1150	
1077	1075	
1025	1025	
893	891	

From the ATR spectra and the peak assignments it is evident that while all other peaks remaining the same for both the films, it was observed that the peak appearing at 1371 cm<sup>-1</sup> for the blank Ch-film was found to appear at 1374 cm<sup>-1</sup> with reduced intensity. Furthermore, the peak appearing at 1259 cm<sup>-1</sup> for the blank Ch-film was found to be absent for Ch-SO<sub>3</sub>Na-CDs nanocomposite films. Also, the peak corresponding to appearing at 1199 cm<sup>-1</sup> for blank Ch-film was found to be shifted to 1150 cm<sup>-1</sup> after incorporation of MUA-SO<sub>3</sub>Na-CDs i.e for Ch-SO<sub>3</sub>Na-CDs nanocomposite films. All these observations make way to provide evidence for the successful incorporation of MUA-SO<sub>3</sub>Na-CDs into the chitosan hydrogel matrix via electrostatic interaction.

Figure S5 (B) shows the stacked TGA thermograms of Ch-SO<sub>3</sub>Na-CDs nanocomposite films and Blank Ch-films. From the graphs it is observed that the blank Ch-film and Ch-SO<sub>3</sub>Na-CDs nanocomposite film undergoes degradation at two stages viz. at 272°C and 532°C. However, the interesting fact to be noticed is that after incorporation of MUA-SO<sub>3</sub>Na-CDs into the chitosan hydrogel matrix, the Ch-SO<sub>3</sub>Na-CDs nanocomposite films undergo somewhat lesser extent of degradation compared to the blank Ch-films. It was observed that at 272°C and 532°C while the blank Ch-film undergo 30.7% and 31% degradation, the Ch-SO<sub>3</sub>Na-CDs nanocomposite films undergo only 24% and 28% degradation respectively. Thus, it is clear that the Chitosan films acquire greater thermal stability upon formation of nanocomposites with MUA-SO<sub>3</sub>Na-CDs thereby indicating successful incorporation of the CDs into the hydrogel matrix.

### **7. Removal of Ca<sup>2+</sup> from aqueous solution by Ch-SO<sub>3</sub>Na-CDs nanocomposite film**

The millivolt potentials of standard solutions of Ca<sup>2+</sup> (10<sup>-5</sup>, 10<sup>-4</sup>, 10<sup>-3</sup>, 10<sup>-2</sup> and 10<sup>-1</sup>M) were measured using a Calcium Combination Ion Selective Electrode in an Accumet Excel Dual

Channel pH/Ion/Conductivity Meter, XL 50 (Fischer Scientific). The electrode was immersed into the standard solutions and the millivolt readings were recorded once it has attained stabilization. Subsequently a calibration curve was constructed by plotting the concentration of  $\text{Ca}^{2+}$  on the X-axis and the corresponding millivolt reading on the Y-axis. The data was then fitted logarithmically to obtain the calibration curve as shown in the main manuscript (Figure 2(A)). The potential of the sample solution (unknown) was then measured in a similar way under identical conditions. The concentration of the unknown (the solution of  $\text{Ca}^{2+}$  after dipping-in of the Ch- $\text{SO}_3\text{Na}$ -CDs nanocomposite film and blank chitosan film) was then determined by using the mV reading and plotting it in the equation obtained from logarithmic fitting of the standard data. Likewise the concentrations of  $\text{Ca}^{2+}$  were determined at different time intervals starting from 0<sup>th</sup> hour to 24<sup>th</sup> hour (although the time interval monitored was upto 60<sup>th</sup> hour, significant absorption of  $\text{Ca}^{2+}/\text{Mg}^{2+}$  took place within 24 hours and therefore the plot of  $\text{Ca}^{2+}/\text{Mg}^{2+}$  removal has been shown upto 24 hours) and the concentration values were plotted against the time interval to obtain the plot as shown in Figure 2(B) (main manuscript). This procedure was followed for both samples with dipped-in Ch- $\text{SO}_3\text{Na}$ -CDs nanocomposite film and blank chitosan film. From the plot it is evident that the decrease in  $\text{Ca}^{2+}$  concentration in solution is faster and higher for solutions with dipped-in Ch- $\text{SO}_3\text{Na}$ -CDs nanocomposite films as compared to those with dipped blank Ch-films thereby focusing the role played by the sulphonated CDs ( $\text{SO}_3\text{Na}$ -CDs) embedded in the nanocomposite film in  $\text{Ca}^{2+}$  removal.

According to WHO report the Water hardness as classified by the U.S. Department of Interior and the Water Quality Association is as follows:

<b>Classification</b>	<b>mg/L or ppm</b>
Soft	0 – 17.1
Slightly hard	17.1 – 60
Moderately hard	60-120
Hard	120-180

Very hard	180 and over
-----------	--------------

For consistency, concentrations are generally converted to the equivalent concentration as  $\text{CaCO}_3$  and expressed in terms of hardness as  $\text{CaCO}_3$ . However, Magnesium in hard water limits to 50 ppm. In our case we have used  $5 \times 10^{-4}$  M solutions of Calcium chloride ( $\text{CaCl}_2$ ) and Magnesium chloride ( $\text{MgCl}_2$ ) for our experiments which is equivalent to 20.035 ppm of  $\text{Ca}^{2+}$  and 12.15 ppm of  $\text{Mg}^{2+}$ . These values fall within the range where the water can be considered as slightly hard as evident from the above table. Therefore, we think that it is quite logical to consider this concentration for the experimental design that we present herein.

### **8. Removal of $\text{Mg}^{2+}$ from aqueous solution by Ch- $\text{SO}_3\text{Na}$ -CDs nanocomposite film**

In order to study the possible effect of other ions such as  $\text{Mg}^{2+}$  usually co-present with  $\text{Ca}^{2+}$  in water we carried out the experiment for a mixture of both  $\text{Ca}^{2+}$  and  $\text{Mg}^{2+}$  in solution.  $5 \times 10^{-4}$  M solutions each of  $\text{CaCl}_2$  and  $\text{MgCl}_2$  were prepared and mixed together. 2cm x 2cm Ch- $\text{SO}_3\text{Na}$ -CDs films were dipped in the mixture for 60 hours and the corresponding concentration of  $\text{Ca}^{2+}$  and  $\text{Mg}^{2+}$  were determined using a Calcium Combination Ion Selective Electrode and also via Atomic Absorption Spectroscopy (AAS) respectively. The initial concentrations (zeroth hour) of  $\text{Ca}^{2+}$  and  $\text{Mg}^{2+}$  in solution were equivalent to 20.039 ppm and 12.150 ppm respectively. After dipping in of the Ch- $\text{SO}_3\text{Na}$ -CDs films (at the end of 24<sup>th</sup> hour) the concentration of  $\text{Ca}^{2+}$  was found to be 6.812 ppm as determined using the Calcium Combination Ion Selective Electrode. Further, the concentration of  $\text{Mg}^{2+}$  was found to be 3.50 ppm (24<sup>th</sup> hour) as obtained from Atomic Absorption Spectroscopy. Therefore, from this experiment it is very well evident that the Ch- $\text{SO}_3\text{Na}$ -CDs films prepared could effectively remove both  $\text{Ca}^{2+}$  and  $\text{Mg}^{2+}$  from solution in the pure state and even when they are present together in a mixture.

### **9. Analysis of Pond Water Sample**

The potential applicability of the chitosan-sulphonated carbon dot nanocomposite as an efficient ion-exchange film for removal of Calcium and Magnesium from real environment water sample has been successfully tested. Water sample was collected from a local area pond and filtered using ordinary filter paper to remove all suspended matter. The presence of Calcium and Magnesium in the sample was confirmed via measurement using Calcium Combination Ion Selective Electrode in an Accumet Excel Dual Channel

pH/Ion/Conductivity Meter, XL 50 (Fischer Scientific) and Atomic Absorption Spectroscopy (AAS) respectively. After that 2cm x 2cm pieces of the chitosan-sulphonated carbon dot nanocomposite film were cut and dipped in the samples and allowed to stand for 24 hours. The procedure for detection of Calcium by the Calcium ion-selective electrode and Magnesium by Atomic Absorption Spectroscopy (AAS) were performed as described earlier. It was found that the pond water sample contained 20.198 ppm of  $\text{Ca}^{2+}$  and 3.2617 ppm of  $\text{Mg}^{2+}$  before dipping of the nanocomposite film. After dipping of the chitosan-sulphonated carbon dot nanocomposite film the respective concentrations were found to be 6.4613 ppm ( $\text{Ca}^{2+}$ ) and 1.4237 ppm ( $\text{Mg}^{2+}$ ) in solution. It was observed that the removal of Ca and Mg from the real sample by the nanocomposite film was found to be quite satisfactory. The histogram plot for the Calcium and Magnesium removal from the real sample by the film is shown in Figure 2(D)(ii) in the main manuscript. From the plot it is seen that the percentage removal of Calcium and Magnesium from pond water by the nanocomposite film was 68.01% and 56.35% respectively. Therefore the material developed has potential applicability as a water softener based on the principle of ion-exchange.